Accepted Manuscript

Characterization and electrochemical properties of organomodified and corresponding derived carbonized clay

N. Jović-Jovičić, M. Mojović, D. Stanković, B. Nedić-Vasiljević, A. Milutinović-Nikolić, P. Banković, Z. Mojović

PII: S0013-4686(18)32503-9

DOI: https://doi.org/10.1016/j.electacta.2018.11.031

Reference: EA 33032

To appear in: *Electrochimica Acta*

Received Date: 12 June 2018

Revised Date: 17 September 2018

Accepted Date: 5 November 2018

Please cite this article as: N. Jović-Jovičić, M. Mojović, D. Stanković, B. Nedić-Vasiljević, A. Milutinović-Nikolić, P. Banković, Z. Mojović, Characterization and electrochemical properties of organomodified and corresponding derived carbonized clay, *Electrochimica Acta* (2018), doi: https://doi.org/10.1016/j.electacta.2018.11.031.

This is a PDF file of an unedited manuscript that has been accepted for publication. As a service to our customers we are providing this early version of the manuscript. The manuscript will undergo copyediting, typesetting, and review of the resulting proof before it is published in its final form. Please note that during the production process errors may be discovered which could affect the content, and all legal disclaimers that apply to the journal pertain.

View metadata, citation and similar papers at core.ac.uk

brought to you by CORE

provided by Central Repository of the Institute of Chemistry, Technology and Metallurgy (CER)

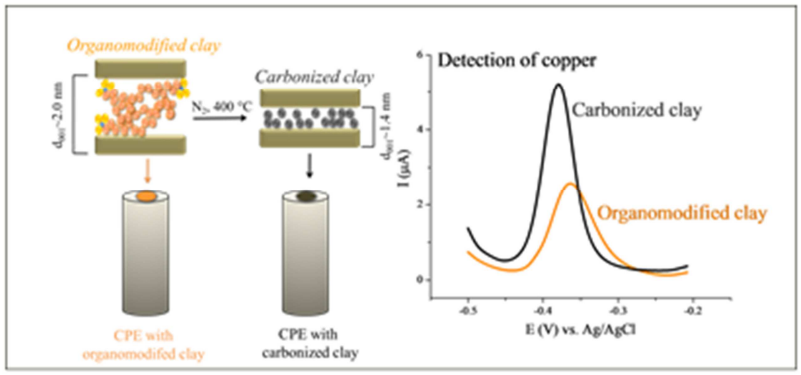

ACCEPTED MANUSCRIPT

ACCEPTED MANUSCRIPT

Characterization and electrochemical properties of organomodified and corresponding derived carbonized clay

N. Jović-Jovičić[a], M. Mojović[b], D. Stanković[c,d] , B. Nedić-Vasiljević[b], A. Milutinović-Nikolić[a], P. Banković[a], Z. Mojović[a*]

[a] *University of Belgrade, Institute of Chemistry, Technology and Metallurgy, Department of Catalysis and Chemical Engineering, Njegoševa 12, 11000 Belgrade, Republic of Serbia*

[b] *Faculty of Physical Chemistry, University of Belgrade, Studentski trg 12-16, P.O.Box 47, 11158 Belgrade, Serbia*

[c]*The Vinca Institute of Nuclear Sciences, University of Belgrade, POB 522, 11001 Belgrade, Serbia*

[d] *Department of Analytical Chemistry, Innovation Center of the Faculty of Chemistry, University of Belgrade, Studentski trg 12-16, Belgrade 11000, Serbia*

ACCEPTED MANUSCRIPT

* Corresponding author: E-mail: zoricam@nanosys.ihtm.bg.ac.rs; Phone: +381 11 2630213; Fax: +381 11 2637977

ACCEPTED MANUSCRIPT

Abstract

Series of alkylammonium modified smectites with different alkylammoinum/clay ratios was synthesized (H series). The obtained organoclays were used as precursors for carbon-clay composite materials (C series). Both set of materials were characterized by X-ray diffraction (XRD), point of zero charge (pH_{PZC}), N_2 adsorption-desorption isotherms, Raman spectroscopy and electron paramagnetic resonance (EPR) analysis.

XRD analysis of organomodified clays confirmed incorporation of $HDTMA^+$ into interlamellar space of smectite. Series of carbonized clays showed constant d_{001} value of 1.4 nm. The pH_{PZC} of two series differed indicating that carbonization changed the profile of pH dependent sites on the clay surface. Textural properties of the H series decreased throughout the series, while in the C series the most developed porous structure was obtained for sample where $HDTMA^+$ loading was equal to cation exchange capacity. Raman spectroscopy showed that amorphous carbon was formed during carbonization process.

The obtained materials were used as modifiers of carbon paste electrode and investigated using electrochemical impedance spectroscopy, cyclic voltammetry and square wave voltammetry. The comparison of electrochemical behavior of H series and C series showed the importance of interlamellar species for charge transfer process. The investigation of influence of composition of carbon paste and form of added carbon showed that performance of carbon-clay based electrodes depended on synergy of different factors.

Keywords: smectite; organomodified clay; carbonized clay; carbon paste electrode

ACCEPTED MANUSCRIPT

1. Introduction

Carbon based materials represent interesting research area due to their applicability in various fields of industry. Graphite is a form of carbon that was first that find extensive application in industry and biomedical engineering. Various types of carbon based nanomaterials such as single and multiwalled nanotubes, fullerenes, nanodiamonds and graphene were developed during last decades [1]. Advantageous properties of these materials such as high electrical and thermal conductivity, mechanical strength etc., were explored and used for various applications [2]. However, the price of these materials is an obstacle for their extensive industrial usage. Therefore, new synthetic routes and new carbon composite materials are developing.

One of pathway is usage of phylosilicates as templates for graphite-like materials preparation [3, 4]. The investigation involved two approaches, elimination of inorganic host by acid treatments in order to obtain carbonaceous material or preparing of supported carbon material on silica or silicate solids [5-13]. Ruiz-Hitzky et al. [14-16] investigated obtaining of graphene-like materials supported on porous solids using ecological compatible resources, such as the sucrose disaccharide and the gelatin protein.

The precursor for carbon-clay composite material is usually organomodified clay. The organically modified clays have found their application in electrochemistry as solid electrodes and biosensors [16], as well as clay polymer electrolytes [17, 18]. In our previous studies [20-22] we have used alkylammonium ions for modification of bentonite-clay rich in smectite. The obtained organomodified-smectites were used as part of composite electrode for determination of phenol and nitro-phenol compounds. Electrodes based on clay modified with surfactant have also been investigated by other groups [23, 24]. Group of Ngameni and Tonle has intensively investigated electroanalytical applications of surfactant modified clays with inorganic [25, 26]

and organic [27-30] species. The ion-exchange reaction, used for intercalation of alkylammonium ions in interlamellar spaces of smectite, enables easy control of alkylammonium ion/clay ratio. This ratio has significant influence on electrochemical performance of the obtained materials [22].

In this article, we present study of carbon-clay composites obtained by carbonizing hexadecyltrimethylammonium (HDTMA) modified clays. The domestic bentonite clay (from locality Bogovina, Serbia) was modified with different amounts of $HDTMA^+$ in order to obtain composites with different carbon/clay ratios. The aim of this investigation was to test the influence of carbon content on properties of composites. The materials, both parental organomodified clays and carbonized clays derived from them, were characterized by different techniques. The both sets of materials were used as modifier of carbon paste electrode in order to test the changes in their electrochemical properties. The activity of formed carbon-clay composite toward cation sensing was investigated. The comparison with parental organoclay activity was used to provide the insight of the role of intercalated species in the activity of investigated composites. Carbon-clay composites can provide combination of properties that can enhance the performance of paste electrode modified by them.

2. Experimental

The preparation of samples is presented in more details in our previous publication [22]. In short, Na-enriched bentonite (Na-B) was prepared from the bentonite fraction (<74 μm). Clays with different HDTMA loadings were obtained by varying of HDTMA/Na-B ratios in batch suspension. The appropriate HDTMA-Br/bentonite ratios were used in order to obtain clay modified with 0.2, 0.5, 1.0, 2.0 and 3.0 times of cation exchange capacity (CEC) value. These

materials are referred as samples of H series with each sample having a number indicating multiples of CEC i.e. 0.2H, 0.5H, 1.0H, 2.0H and 3.0H.

The obtained organomodified clays were heated under nitrogen atmosphere with heating rate of 10 °C/min until 400 °C was reached. The temperature was held on 400 °C for 30 minutes. After that, samples were cooled down to the room temperature under nitrogen atmosphere. The samples were designated after corresponding parental material as 0.2C, 0.5C, 1.0C, 2.0C and 3.0C. These materials are referred as samples of C series.

The XRD analysis was performed using a Philips PW 1710 X-ray powder diffractometer with a Cu anode (λ = 0.154178 nm). The XRD patterns were obtained in the 2θ range of 3–50 ° with 0.02 ° step for all investigated samples.

Batch equilibration technique [31] was employed for determination of the point of zero charge (pH_{PZC}) for all samples. The initial pH values (pH_i) of sample dispersions were adjusted in the pH range from 2 to 12 by adding 0.1 M HCl or 0.1 M NaOH solution. The dispersions were shaken for 24 h, followed by centrifugation and the measurement of final pH (pH_f). The pH_{PZC} was determined from pH_i vs. pH_f diagram. The pH of the solution was monitored using a "Jenway" 3320 pH meter.

Nitrogen adsorption–desorption isotherms were determined using a Micromeritics ASAP 2020 instrument. Samples were degassed at 150 °C for 10 h under reduced pressure. The specific surface area of samples was calculated according to the Brunauer, Emmett, Teller (BET) method from the linear part of the nitrogen adsorption isotherms [32]. The total pore volume (V_{tot}) was given at p/p_0 = 0.998. The volume of the mesopores was calculated according to the Barrett, Joyner and Halenda method from the desorption branch of isotherm [33]. The volume of micropores was calculated from alpha-S plot [32].

Raman spectra were recorded using DXR Raman Microscope (Termo Scientific) and 532 nm excitation wavelength. Measurements were made using 50 µm slit aperture and standard working distance objective 10x, with the power of illumination at the sample surface of 10 mW. The acquisition time was 10 s with 30 scans. Thermo Scientific OMNICTM software was used for spectra acquisition and analysis.

The electron spin resonance (ESR) spectra of the powder samples were recorded at room temperature by a Bruker Elexsys IIE540 spectrometer operating at X-band (9.5 GHz) with the following settings: modulation amplitude 2 G; modulation frequency 100 kHz; microwave power 6.3 mW; scan range 514 mT; scan time 4 min. The spectra were recorded and analyzed using the Xepr software (Bruker BioSpin Germany).

Carbon black paste was prepared by hand mixing 0.5 g of carbon black (CB) (Vulcan-XC 72R) with 0.5 g of paraffin oil. High amount of paraffin oil was necessary to apply due to high surface area (254 m^2/g) and pore volume (174 $cm^3/100$ mg) of the used carbon black [34]. The resulting paste was packed into the hollow (1 mm diameter) Teflon tube while the electrical contact was provided using copper wire and the obtained setup was used as working electrode. For comparison purpose the pure carbon black paste (without modifier) was tested and designated as CBP. Carbon pastes with the clay samples as modifiers were prepared with two different CB/clay ratios. The first ratio (CB/clay = 2:1) was used in order to obtain data for comparison of properties of both sets of clay samples i.e. clay modified with HDTMA and carbon-clay composites. The second ratio (CB/clay = 1:9) was used to investigate carbon-clay composites in order to test the ability of carbon formed *in situ* to provide good electrical contact. The electrodes formed with different CB/clay ratio were denoted as 2:1 and 1:9 electrodes. Additional electrodes were made in order to test the role of form of added carbon in paste

electrodes. Graphite based paste electrode (GPE) was made by hand mixing 0.5 g graphite with 0.15 g paraffin oil. Pure 1.0C electrode (without additional carbon) was made by hand mixing 0.5 g 1.0C sample with 0.2 g paraffin oil. Finally, 1.0C GPE was made by hand mixing 1.0C and graphite in graphite /clay = 1:9 ratio with paraffin oil.

The reference electrode was Ag/AgCl in 3 M KCl, while a platinum rod served as a counter electrode. The electrochemical measurements were performed using Autolab electrochemical workstation (Autolab PGSTAT302N, Metrohm-Autolab BV, Netherlands). Impedance measurements were carried out at open circuit potential (OCP) using a 5 mV rms sinusoidal modulation in the 10 kHz–10 mHz frequency range. The 5 mM $K_4[Fe(CN)_6]$ in 0.5 M KCl was used as electrolyte. Cyclic voltammetry was performed at scan rate of 50 mVs^{-1} using the same electrolyte. Square wave voltammetry was used for investigation of the electrode response toward Cu(II). First Cu(II) was accumulated on the investigated electrodes from magnetically stirred solution of 0.01 M Cu(II) for 2 minutes at pH=5.5. After accumulation, each electrode was rinsed with water and dried with paper. The electrode was then transferred in electrochemical cell containing 0.1 M HCl that served as stripping solution. Reduction of accumulated Cu (II) was performed at potential of -0.9 V for 60 s. Finally, the determination of copper was performed by square wave voltammetry immediately after the reduction step. The square wave voltammograms (SWV) were recorded in the potential window of -0.5 V to -0.2 V vs. Ag/AgCl electrode with following parameters: pulse amplitude = 20 mV, scan increment = 10 mV and frequency = 10 Hz.

3. Results and Discussion

3.1 XRD

The results of XRD analysis for both series are presented in Fig. 1.

Figure 1

The following crystalline phases were identified [35, 36]: smectite, quartz, feldspar and calcite. The modification with $HDTMA^+$ affected only smectite. The incorporation of $HDTMA^+$ into interlamellar space resulted in the increase of d_{001} value of smectite. According to literature [37, 38] d_{001} value of 1.4 nm, 1.8 nm, 2.0 nm and 2.2 nm correspond to mono-molecular layer, bi-molecular layer, pseudo-trimolecular layer and paraffin type of layer, respectively. The obtained values indicate formation of monolayer for 0.2H, both monolayer and bilayer for 0.5H and pseudo-trimolecular layer for 1.0H. When the loading of $HDTMA^+$ exceeded CEC the peak corresponding to d_{001} = 2.0 nm persist to exists, indicating possibility of the existence of pseudotrilayer arrangement of $HDTMA^+$. According to literature, d_{001} value for samples with $HDTMA^+$/CEC ratio in the interval from 2.0 to 4.0, are between 2.95-4.03 nm [38-40] and are registered by low-angle (2θ = 1–3°) XRD analysis. The obtained values indicated the presence of paraffin layer not excluding the partial presence of pseudotrilayer arrangement [41-43]. Therefore, the obtained peak at 2θ=4.43 ° might correspond to the (002) reflection and basal spacing of 4.0 nm. Also, the peaks at 6.85 ° and 15.97° could be the (003) and (007) reflections, respectively corresponding to basal spacing of 3.87 nm that is also within interval that is in agreement with literature [38-40]. These peaks are more pronounced in 3.0H in comparison to 2.0H confirming the increased incorporation of $HDMA^+$ into smectite structure.

In the sample 0.2C obtained by carbonizing the clay with the smallest amount of $HDMA^+$ the collapse of layered structure of smectite occurred characteristic for heat treated unmodified clays [44]. The presence of amorphous carbon on the clay surface with wide peak in interval 14-37 ° of 2θ [45] was not able to be detected due to presence of the more expressed crystalline structures i.e. smectite and quartz. The samples obtained by carbonizing clays with $HDMA^+$/CEC ratios in

interval 0.5-3.0 was d_{001}=1.4 nm regardless the loading. Different authors reported d_{001} values for carbonized clays previously intercalated with various organic species in range between 1.1-2.2 nm [46,51]. The thickness of carbon layer was not straightforward determined by the amount of organic phase. According to these literature data the obtained thickness depended on the type of the applied clay and organic precursor. Among mentioned only P. Anadão et al. [49] reported the carbonized clays with different loading of source of carbon. In their study the d_{001} was the same regardless loading.

3.2 PZC

The dependence of pH_f on pH_i in pH range 2-12 was investigated for all samples. The results obtained for samples Na-B, 3.0H, 0.2C and 3.0C are given in Fig. 2.

Figure 2

There are two types of charge sites in clay minerals including smectites [37]: pH dependent sites and pH independent structural sites. pH independent charge sites are the result of isomorphic substitution in the clay structure, and their charge will not be changed with the change of pH of electrolyte. pH dependent sites originate from terminal OH groups located at broken edges, steps and other crystalline defects. The sign of these under-coordinated OH groups will change depending on the pH value of the electrolyte.

The point of zero charge is the pH value where the net surface charge is zero. The point of zero charge (pH_{PZC}) of two series differed while within the same series it was almost constant. Therefore, for clarity sake the results obtained for other samples within series are omitted from graph. As previously reported [52] the Na-B and series of HDTMA-bentonites had broad plateau (approx. from pH≈5 to pH≈10) with $8.3 \leq pH_{PZC} \leq 8.8$. On the other hand, the carbonized clays had narrow plateau with pH_{PZC}=6.7±0.2. This plateau was in the range from pH≈6 to pH≈8 for

0.2C and steadily narrowing with the increase of $HDTMA^+$ loading in parental clay. This trend resulted in absence of plateau on graph for 3.0C where only inflection point at pHi=7.5 and pHf=6.5 was detected.

The presence of HDTMA slightly shifted pH_{PZC} toward higher pH values. This effect was somewhat more expressed for the organobentonites where the loading exceeded CEC value. The excess of HDTMA ions is dominantly bounded by hydrophobic interaction in interlamellar layer, but it can also be partially bounded to the edges of clay particle [53]. Thus, adsorption of alkylammonium cations for these samples is accompanied by desorption of protons from surface OH groups that lead to subsequent decrease of the amount of pH dependent charge sites on the edges. Therefore, the pH_{PZC} of HDTMA clays was shifted slightly to the basic pH.

Upon calcination, the pH_{PZC} was shifted to more acidic pH and pH_{PZC} values determined for the C series were close to the pH_{PZC} value obtained for the pH_{PZC} of edges of smectite [13,54].

The plateau in the plots presented in Fig. 2 represents the pH range where investigated material acts as buffers [55]. The ability of carbonized clay to act as buffer decreased within the C series, indicating that terminal hydroxyl groups, responsible for buffer-like response, were permanently blocked by carbon. The changes in interlamellar space were also evidenced by the EPR analysis (Fig S2 of Supplementary data).

3.3 Textural properties

The nitrogen adsorption–desorption isotherms of Na–B and both H and C series are shown in Fig. S1 of Supplementary data. The textural properties calculated from these isotherms are presented in Table 1.

Table 1

Values of all textural properties of the H series decreased with the increase of the surfactant loading. Passage of the probe molecule (nitrogen) was inhibited by the presence of HDTMA cations responsible for pore blockage. In the C series the highest value of specific surface area and pore volume was obtained for 1.0C sample. Diminishing of textural properties was noticed with the increase of HDTMA loading above CEC in parental clay. The least developed porous structure in C series was found for 0.2C and 0.5C.

3.4 Raman spectroscopy

The Raman spectra were recorded (Fig. 3) in the range from 800 to 2400 cm^{-1} in order to avoid intense background noise originated from clay.

Figure 3

The Raman spectra of all carbon-clay composites had well defined line at around 1590 cm^{-1}. This line is usually denoted as G line and corresponds to the bond stretching of sp^2 carbon atoms in both rings and chains [56]. Additional slightly expressed shoulder at around 1390 cm^{-1} appeared in the Raman spectra of samples obtained from organoclays with HDTMA loading equal or higher than CEC. The line at this frequency is noticed only in the presence of disordered carbon structures and is known as D band [57]. The position and the intensity of lines in recorded Raman spectra indicated that amorphous carbon was formed in carbon-clay composites.

3.5 Electrochemical properties

3.5.1 Electrochemical impedance spectroscopy (EIS)

The electrochemical properties of clay modified carbon paste electrode with CB/clay ratio of 2:1 were investigated by EIS experiments. All impedance measurements were performed immediately after immersion of the electrode into the solution. The obtained EIS spectra are presented in Fig. 4.

Figure 4

The significant difference between spectra of samples of H and C series can be observed in the shape of spectra and the value of impedance. Spectra of H series consisted of half-circle and linear part, while spectra of C series consisted only of half-circle. The impedance values of H series were of the order of kΩ, while C series had impedance value of the order of MΩ.

The obtained spectra were fitted with modified Randles circuit (Fig. 5).

Figure 5

Original Randles circuit consists of internal resistance (R_S) in series with the parallel combination of the double-layer capacitance (C_{dl}) and an impedance of a faradaic reaction (serial combination of charge transfer resistance R_{ct} and Warburg impedance). The double-layer capacitance (C_{dl}) is often replaced with a constant phase element (CPE). The CPE represents non-ideal capacitor. The impedance of CPE element is given as:

$$Z = \frac{1}{Y} = \frac{1}{(i\omega)^n Q}$$

where Y is CPE admittance, i is the imaginary unit, ω is the angular frequency, n is CPE exponent which is associated with the system inhomogeneity and Q has the numerical value of the admittance (1/ |Z|) at ω =1 rad/s.

The capacitance element CPE will become pure capacitance, pure resistance and Warburg impedance when n = 1 , n = 0 and n = 0.5, respectively. Therefore, the resistor (R), capacitor (C) and Warburg impedance (W) can be considered to be special cases of CPE [58]. However, even the circuit where the double-layer capacitance C_{dl} was replaced with CPE (in the circuit labeled Q), i.e. circuit ($R_s((R_{ct}W)Q)$), was not applicable for fitting of the experimental data. Instead, the circuit ($R_s((R_{ct}Q_1)Q_2)$) (Fig. 5), where both C_{dl} and W were replaced with CPE, was used to fit obtained EIS spectra. In this circuit, Q_1 and Q_2 were used to describe diffusion

process and electric double layer, respectively. The results obtained using fitting with this circuit are presented in Table 2.

Table 2

The internal resistance, R_s, was almost constant (42 Ω -55 Ω) for all investigated samples of both series. The charge transfer resistance, R_{ct}, decreased with the increase of $HDTMA^+$ content in samples of H series. This finding might indicate the importance of the presence and arrangement of HDTMA in interlamellar space in the electron transfer process. The admittance of diffusion, Y_1, and double layer capacitance, Y_2, increased with the increase of $HDTMA^+$ content. This increase was particularly expressed for samples where the amount of $HDTMA^+$ loading exceeded CEC value. It can be assumed that for 2.0H and 3.0H samples the presence of pseudo-trilayer and/or paraffin arrangement of $HDTMA^+$ favored the $[Fe(CN)_6]^{3-/4-}$ anion adsorption.

The behavior of the C series showed different trends. The charge transfer resistance was almost constant in C series, except for 0.2C sample that showed somewhat lower value. This value was only slightly higher than the one obtained for CBP. Keeping in mind that in 0.2C collapse of layered structure of smectite occurred, all findings regarding 0.2C could be expected to be somewhat different from the rest of C series. The results for admittances Y_1 and Y_2 obtained for C series showed maximum for 1.0C. It can be speculated that the structure, textural properties and the arrangement of charge sites obtained when the amount of carbonized HDTMA was equal to CEC was favorable for both diffusion process and the effect of double layer. The almost constant charge transfer resistance of 1.0C, 2.0C and 3.0C samples probably indicated that almost the same amount of carbon material was present in these samples.

3.4.2 Cyclic voltammetry of $K_4[Fe(CN)_6]$

Further investigation of parental organoclays and carbonized clay materials was performed by cyclic voltammetry from aqueous solution of 1 mM $K_4[Fe(CN)_6]$ in 0.5 M KCl (Fig. 6).

Figure 6

Cyclic voltammograms (CV) recorded for all investigated clay samples including Na-B exhibited pair of peaks corresponding to the oxidation and the reduction peaks of $[Fe(CN)_6]^{3-/4-}$ couple. The presence of response of anionic probe on clay-based material can be unexpected since smectite sheets have permanent negative charge introduced by isomorphic substitution. The question of response of anionic probe on cationic clays has already been noted and discussed by other researchers [59,60]. Although in some experiments the complete absence of response for starting clay was noticed [58], in the other experiments the response was recorded and explained by cationic sites at the edges of clay particles that were available for anion adsorption [60].

The electrochemical parameters (midpoint potential ($E_{1/2}$), peak-to-peak separation (ΔE_p) and anodic to cathodic current ratio Ia/Ic) obtained from the results presented in Fig. 6 are given in Table S1 of Supplementary data.

The value of midpoint potential of $[Fe(CN)_6]^{3-/4-}$ couple was almost constant through H series and only for 3.0H decreased value was recorded. It can be assumed that reaction on 3.0H electrode was more thermodynamically favorable in comparison to other electrodes. Navratilova et al. [23] also noted the beneficial effect of low HDTMA concentration in solution and ascribed to micellar effect of HDTMA. The noticed decrease of $E_{1/2}$ in this work corroborates with the structure of 3.0H where probably a part of $HDTMA^+$ was weekly bonded to clay structure and therefore readiest to be dissolved into the supporting electrolyte. The concentration of released

$HDTMA^+$ in the pre-electrode solution composition was probably sufficient to express micellar effect and affect $E_{1/2}$. Furthermore, the I_a/I_c ratio converge to unity with the increase of $HDTMA^+$ content in sample indicating better retention of formed $[Fe(CN)_6]^{3-}$ at the electrode surface. This effect can be ascribed to the accumulation of the negatively-charged probes by the positively-charged surfactant [17]. The peak-to-peak separation was relatively constant in H series, exhibiting more expressed variations for samples where the HDTMA loading was ≥ CEC value.

All carbon-clay composite based electrodes showed CV similar to unmodified CBP with high ΔE_p values indicating slow kinetics. ΔE_p values decreased with the increase of $HDTMA^+$ loading in parental clay. This decrease was the highest for 3.0C and ΔE_p was for 0.15V lower than for CBP. This finding indicated that carbon formed *in situ* had beneficial effect on the electrochemical reversibility of the composite electrodes. Nevertheless, ΔE_p values for entire C series were significantly higher in comparison to those for samples of H series. The I_a/I_c ratio recorded at electrode modified with carbonized clays was above 1 due to low cathodic current indicating low retention of formed $[Fe(CN)_6]^{3-}$ at the electrode surface.

3.4.3 Square wave voltammetry of Cu(II)

The further comparison of HDTMA-modified clays and carbonized clay derived from them was performed by investigating their activity toward positive ion, Cu(II). The investigation was carried out by method of striping square wave voltammetry. The anodic peak corresponding to oxidation of previously adsorbed and reduced Cu(II) was observed in potential range from -0.38 to -0.31 V vs. Ag/AgCl (Fig. 7).

Figure 7

The highest current response was observed for starting Na-B sample. With the increase of $HDTMA^+$ content in H series the current response from Cu decreased that is in accordance with

literature data [23]. The possible Cu(II) sorption sites in HDTMA-modified smectite were occupied with alkylammonium cations, that resulted in current decrease. Furthermore, the peaks recorded using 2.0H and 3.0H based electrodes were poorly resolved and shifted toward more positive potential. The value of peak current was comparable to the value obtained for unmodified CBP (around 0.1 μA), indicating that these samples provide little or no contribution to the current response. Similar values of peak currents were obtained for electrodes based on corresponding samples of each of series (Fig. S3 of Supplementary data). Difference between two series was noticeable for samples 2.0C and 3.0C, since the recorded signals for these electrodes expressed clearly defined peak, although with low peak currents (around 0.3 μA) and at higher potentials.

The obtained results indicated that the number of available sites for adsorption of cations influenced detection of cationic species. The electrochemical response of clay-based electrode is known to be dependent on the accumulation of analyte by ion-exchange [17]. Preconcentration of copper ions is enabled by cation exchange property of smectite structure. The increase of HDTMA loading declined both cation exchange capacity and porosity of clay that resulted in the lower copper oxidation current. In C series the residual carbon material that remained in clay after carbonization acted in similar manner. Samples 2.0C and 3.0C showed better electrochemical response than their parental clay samples. This feature might be attributed to the higher porosity of 2.0C and 3.0C samples in comparison to corresponding organoclay samples.

3.4.4 The influence of carbon paste composition

The electrochemical response of carbon paste electrodes depends on their composition. It was previously suggested that carbon modified materials similar to materials of C series investigated in this paper, could be prepared as carbon paste electrode without added carbon [13]

used to enhance electric contact. Since samples of C series contained various amounts of carbon it was decided to add 10 wt. % of carbon black (i.e. the electrodes were formed with CB/clay ratio of 1:9). Nyquist plot obtained for electrodes prepared in this manner are presented in Fig. 8.

Figure 8

The obtained spectra were fitted with the same circuit as previously given (Fig. 5) i.e. ($R_s((R_{ct}Q_1)Q_2)$). The internal resistance, R_s, was almost constant but increased several dozen times in comparison to the electrode formed with CB/clay ratio of 2:1 and was in the range 2.5-3.0 kΩ. The internal resistance (R_s), that includes ionic resistance of electrolyte, inherent resistance of active material, and contact resistance at the interface of active material-current collector, can be found as the first intersecting point with the real axis in the high-frequency region [61]. Since the internal resistance highly depends on conductivity of bulk material [62] it can be concluded that reduced amount of carbon black in carbon paste electrode resulted in increased R_s.

In contrast to this result, the values of charge transfer resistance (Table 2) were several times lower than values obtained for electrode formed with higher amount of carbon black (Table 1).

Table 2

These lower values indicated more efficient electron transfer process. Possible explanation can be that carbon formed *in situ* has significant role in the electrode performance, as previously reported [13].

The results of cyclic voltammetry of $K_4[Fe(CN)_6]$ on composite electrodes formed with CB/clay ratio of 1:9 are summarized in Table S2 of Supplementary data. The value of $E_{1/2}$ for $[Fe(CN)_6]^{3-/4-}$ couple was shifted toward more positive values for 1:9 electrodes in comparison to 2:1 electrodes. The rate of charge transfer was higher than with the electrode prepared with the

excess of carbon black indicated by ΔE values lower for about 0.2 V. The redox behavior of $[Fe(CN)_6]^{3-/4-}$ couple is sensitive to the surface chemistry, microstructure and electronic properties of the electrode [63]. The electrochemistry of inner-sphere redox probe, such as $[Fe(CN)_6]^{3-/4-}$ couple, usually involves specific adsorption of the reactants, intermediates, or products on the electrode surface [64]. It can be summarized that the influence of surface properties of carbonized clays in 1:9 electrodes was more significant for electrode behavior than in 2:1 electrodes.

The investigation of sensitivity of the 1:9 electrodes toward Cu(II) showed that their behavior was different than the behavior of 2:1 electrodes. All voltammograms of C samples exhibited well defined peak (Fig. 9).

Figure 9

The highest peak current was recorded for 1.0C sample at lowest peak potential. In order to emphasize the influence of carbon paste electrode composition, peak currents recorded with electrodes having different CB/clay ratios are given in Fig. S4 of Supplementary data. The electrodes having CB/clay ratio of 1:9 had better electrochemical response for all samples whose paternal clay had the amount of introduced $HDTMA^+$ equal or higher than CEC value.

The influence of form of carbon in paste electrodes was tested by comparison with graphite based paste electrode. The sensitivity toward Cu(II) was investigated for graphite paste electrode (GPE), pure 1.0C electrode (without additional carbon) and 1.0C with addition of 10% of graphite (1.0C GPE). The obtained square wave voltammograms are presented in Fig. S5 of Supplementary data. The peak current of GPE was comparable with peak current of CBP and pure 1.0C. The addition of graphite to 1.0C increased response current by 5 times in comparison to pure 1.0C, although the obtained currents were significantly lower in comparison to current

obtained for 1.0C carbon black paste electrode (Fig 7b). The obtained lower currents for 1.0C GPE could probably be ascribed to low dispersity of graphite that led to the poor contact between clay particles and carbon. Good performance of 1.0C carbon black paste electrode might be a consequence of combination of several effects: carbon formed *in situ*, textural properties, ion-exchange capacity and good contact between clay particles and carbon black.

4. Conclusion

Hexadecyl trimethylammonium-modified clays (H series) were synthesized with the aim to be used as precursors for carbon-clay composite materials (C series). Both sets of materials were characterized by XRD, point of zero charge, low temperature N_2 physisorption, Raman spectroscopy and EPR methods. XRD confirmed incorporation of $HDTMA^+$ into interlamellar space of smectite. With the increase of $HDTMA^+$ loading the formation of mono, bi and pseudo-tri layers of $HDTMA^+$ in interlamellar space was confirmed. The samples obtained by carbonizing clays with $HDMA^+$/CEC ratios in interval 0.5-3.0 preserved smectite structure having d_{001}=1.4 nm. The point of zero charge (pH_{PZC}) of two series differed while within the same series it was almost constant. The H series had pH_{PZC} value in the range $8.3 \leq pH_{PZC} \leq 8.8$, while the C series had pH_{PZC}=6.7±0.2. Textural properties of the H series decreased with the increase of the surfactant loading. In the C series the highest value of specific surface area and pore volume was obtained for 1.0C sample. Raman spectroscopy confirmed formation of amorphous carbon in carbon-clay composites. The EPR spectra of all investigated samples showed two main lines at g = 4.23 and g = 2.00, ascribed to structural iron and non-structural iron, respectively.

Electrochemical impedance spectroscopy and cyclic voltammetry of $Fe(CN)_6^{3-/4-}$ redox couple showed that samples of H series had lower charge transfer resistance and better electrochemical

reversibility than samples of C series. The impedance values of H series were of the order of kΩ, while C series had impedance value of the order of MΩ. ΔE_p values for $Fe(CN)_6^{3-/4-}$ redox couple for samples of H series were around 0.1 V, while for samples of C series were around 0.7 V. These results pointed out that interlamellar species play significant role in the charge transfer process. Square wave voltammetry of Cu(II) showed that peak current decreased with the increase of extent of modification along both series due to decreased ion-exchange capacity and porosity. The investigation of influence of composition of carbon paste showed that samples of C series showed better electrochemical response when carbon paste was composed with carbon black/clay ratio of 1:9 than with ratio of 2:1. The best response for detection of Cu(II) was obtained for carbonized sample with HDTMA/CEC=1. Comparison with graphite based paste electrode revealed that performance of carbon-clay based electrode depended on the porosity, ion-exchange capacity, carbon formed *in situ* and good contact between carbon and clay particles.

Acknowledgment: This work was supported by the Ministry of Education, Science and Technological Development of the Republic of Serbia, (Project Nos. III 45001 and III41005). DMS was supported by Magbiovin project (FP7- ERAChairs-Pilot Call-2013, Grant agreement: 621375).

References

[1] C. Cha, S.R. Shin, N. Annabi, M.R. Dokmeci, A. Khademhossein, Carbon-Based Nanomaterials: Multifunctional Materials for Biomedical Engineering, ACS Nano 7(2013) 2891–2897.

ACCEPTED MANUSCRIPT

[2] A. Krüger, Carbon Materials and Nanotechnology. Wiley-VCH: Weinheim, Germany, 2010.

[3] T. Kyotani, N. Sonobe, A. Tomita, Formation of Highly Orientated Graphite from Polyacrylonitrile by Using a Two-Dimensional Space between Montmorillonite Lamellae, Nature 331 (1988) 331-333.

[4] P. Aranda, Clay-Based Polymer Nanocomposites, in: K.A. Carrado, F. Bergaya (Eds), CMS Workshop Lectures Series Vol. 15, The Clay Minerals Society, Chantilly, Virginia, 2007, pp. 171-198.

[5] E. Ruiz-Hitzky, M. Darder, F.M. Fernandes, E. Zatile, F.J. Palomares, P. Aranda, Supported Graphene from Natural Resources: Easy Preparation and Applications, Adv. Mater. 23 (2011) 5250–5255.

[6] E. Ruiz-Hitzky, M.M.C. Sobral, A. Gómez-Avilés, C. Nunes, C. Ruiz-García, P. Ferreira, P. Aranda, Clay-Graphene Nanoplatelets Functional Conducting Composites, Adv. Funct. Mater. 26 (2016) 7394–7405.

[7] C. Nethravathi, B. Viswanath, C. Shivakumara, N. Mahadevaiah, M. Rajamathi, The production of smectite clay/graphene composites through delamination and co-stacking, Carbon 46 (2008) 1773–1781.

[8] C. Santos, M. Andrade, A.L. Vieira, A. Martins, J. Pires, C. Freire, A.P. Carvalho, Templated synthesis of carbon materials mediated by porous clay heterostructures, Carbon 48 (2010) 4049–4056.

[9] P.M. Barata-Rodrigues, T.J. Mays, G.D. Moggridge, Structured carbon adsorbents from clay, zeolite and mesoporous aluminosilicate templates, Carbon 41 (2013) 2231–2246.

[10] D. Gournis, M.A. Karakassides, T. Bakas, N. Boukos, D. Petridis, Catalytic synthesis of carbon nanotubes on clay minerals, Carbon 40 (2002) 2641–2646.

[11] H. Fua, M. Dua, Q. Zhenga, Effect of precursors on the growth of carbon filaments onto clay surface, Appl. Surf. Sci. 257 (2011) 8981–8984.

[12] D. Manikandan, R. V. Mangalaraja, R. Siddheswaran, R. E. Avila, S. Ananthakumar, Fabrication of nanostructured clay–carbon nanotube hybrid nanofiller by chemical vapour deposition, Appl. Surf. Sci. 258 (2012) 4460–4466.

[13] K. Pastorková, K. Jesenák, M. Kadlečíková, J. Breza, M. Kolmačka, M. Čaplovičová, F. Lazištan, M. Michalka, The growth of multi-walled carbon nanotubes on natural clay minerals (kaolinite, nontronite and sepiolite), Appl. Surf. Sci. 258 (2012) 2661–2666.

[14] P. Aranda, M. Darder, R. Fernández-Saavedra, M. Lopez-Blanco, E. Ruiz-Hitzky, Relevance of polymer– and biopolymer–clay nanocomposites inelectrochemical and electroanalytical applications, Thin Solid Films 495 (2006) 104–112.

[15] M. Darder M, E. Ruiz-Hitzky, Caramel–clay nanocomposites. J. Mater. Chem. 15 (2005) 3913–3918.

[16] A. Gomez-Aviles, M. Darder, P. Aranda, E. Ruiz-Hitzky, Functionalized Carbon–Silicates from Caramel–Sepiolite Nanocomposites, Angew. Chem. Int. Ed. 46 (2007) 923–925.

[17] I. K. Tonle, E. Ngameni, A. Walcarius, From clay- to organoclay-film modified electrodes: tuning charge selectivity in ion exchange voltammetry, Electrochim. Acta 49 (2004) 3435–3443.

[18] M. Deka, A. Kumar, Enhanced electrical and electrochemical properties of PMMA–clay nanocomposite gel polymer electrolytes, Electrochim. Acta 55 (2010) 1836-1842.

[19] M. Moreno, R. Quijada, M. A. Santa Ana, E. Benavente, P. Gomez-Romero, G. González, Electrical and mechanical properties of poly(ethylene oxide)/intercalated clay polymer electrolyte, Electrochim. Acta 58 (2011) 112-118.

[20] N. Jović-Jovičić, A. Milutinović-Nikolić, P. Banković, Z. Mojović, M. Žunić, I. Gržetić, D. Jovanović, Organo-inorganic bentonite for simultaneous adsorption of Acid Orange 10 and lead ions, Appl. Clay Sci. 47(2010) 452–456.

[21] A. Milutinović-Nikolić, D. Maksin, N. Jović-Jovičić, M. Mirković, D. Stanković, Z. Mojović, P. Banković, Removal of ^{99}Tc(VII) by organo-modified bentonite, Appl. Clay Sci. 95 (2014) 294–302.

[22] Z. Mojović, N. Jović-Jovičić, A. Milutinović-Nikolić, P. Banković, A. Abu Rabi-Stanković, D. Jovanović, Phenol determination on HDTMA-bentonite-based electrodes, J. Hazard. Mater. 194 (2011) 178–174.

[23] Z. Navrátilová, M. Mucha, Organo-montmorillonites as carbon paste electrode modifiers, J. Solid State. Electrochem. 19 (2015) 2013–2022.

[24] D. Zhou, X. Liu, X. Zheng, Electrochemical determination of phenol using CTAB□ functionalized montmorillonite electrode, Environ Technol 30(7) (2009) 701–706.

[25] G B.P. Ngassa, I. K. Tonlé, A. Walcarius, E. Ngameni, One-step co-intercalation of cetyltrimethylammonium and thiourea in smectite and application of the organoclay to the sensitive electrochemical detection of Pb(II), Appl. Clay Sci. 99 (2014) 297-305.

[26] G B. Ngassa Piegang, I. K. Tonle, A. Walcarius, E. Ngameni, An inorganic-organic hybrid material from the co-intercalation of a cationic surfactant and thiourea withinmontmorillonite layers: application to the sensitive stripping voltammetric detection of Pb^{2+} and Cd^{2+}, C.R. Chimie 19 (2016) 789-797.

[27] J. C. K. Mbouguen, I. K. Tonle, A. Walcarius, E. Ngameni, Electrochemical response of ascorbic and uric acids at organoclay film modified glassy carbon electrodes and sensing applications, Talanta 85 (2011) 754-762.

[28] J. K. Wagheu, C. Forano, P. Besse-Hoggan, I. K. Tonle, E. Ngameni, C. Mousty, Electrochemical determination of mesotrione at organoclay modified glassy carbon electrodes, Talanta 103 (2013) 337-343.

[29] G. B.P. Ngassa, I. K. Tonlé, E. Ngameni, Square wave voltammetric detection by direct electroreduction of paranitrophenol (PNP) using an organosmectite film-modified glassy carbon electrode, Talanta 147 (2016) 547-555.

[30] H. L. Tcheumi, I. K. Tonle, E. Ngameni, A. Walcarius, Electrochemical analysis of methylparathion pesticide by a gemini surfactant-intercalated clay-modified electrode, Talanta 81 (2010) 972-979.

[31] S.K. Milonjić, A.L. Ruvarac, M.V. Šušić, The heat of immersion of natural magnetite in aqueous solutions, Thermochim. Acta 11 (1975) 261–266.

[32] F. Rouquerol, J. Rouquerol, K. Sing, Adsorption by Powders and Porous Slides, Academic Press, London, 1999.

[33] P.A. Webb, C. Orr, Analytical Methods in Fine Particle Technology, Norcross, Micromeritics Instrument Corporation, 1997.

[34] M. Bevilacqua, C. Bianchini, A. Marchionni, J. Filippi, A. Lavacchi, H. Miller, W. Oberhauser, F. Vizza, G. Granozzi, L. Artiglia, S.P. Annen, F. Krumeich, H. Grützmacher, Improvement in the efficiency of an OrganoMetallic Fuel Cell by tuning the molecular architecture of the anode electrocatalyst and the nature of the carbon support, Energy Environ. Sci. 5 (2012) 8608–8620.

[35] International Center for Diffraction Data, Joint Committee on Powder Diffraction Standards (JCPDS), Swarthmore, USA, 1990.

ACCEPTED MANUSCRIPT

[36] N. Jović-Jovičić, A. Milutinović-Nikolić, P. Banković, Z. Mojović, M. Žunić, I. Gržetić, D. Jovanović, Organo-inorganic bentonite for simultaneous adsorption of acid orange 10 and lead ions, Appl. Clay Sci. 47 (2010) 452–456.

[37] F. Bergaya, G. Lagaly, Handbook of clay science, developments in clay science, Amsterdam: Elsevier, 2013.

[38] H. He, R.L. Frost, T. Bostrom, P. Yuan, L. Duong, D. Yang, Y. Xi, J.T. Kloprogge, Changes in the morphology of organoclays with $HDTMA^+$ surfactant loading, Appl. Clay Sci. 31 (2006) 262–271.

[39] J. Zhu, H. He, J. Guo, D. Yang, X. Xie, Arrangement models of alkylammonium cations in the interlayer of HDTMA+ pillared montmorillonites, Chinese Sci. Bull. 48 (2003) 368–372.

[40] H. He, L. Ma, J. Zhu, R.L. Frost, B.K.G. Theng, F. Bergaya, Synthesis of organoclays: A critical review and some unresolved issues, Appl. Clay Sci. 100 (2014) 22–28.

[41] N. Mahadevaiah, B. Vijayakumar, K. Hemalatha, B.S. Jai Prakash, Uptake of permanganate from aqueous environment by surfactant modified montmorillonite batch and fixed bed studies, Bull. Mater. Sci. 34 (2011) 1675–1681.

[42] A. Nuntiya, S. Sompech, S. Aukkaravittayapun, J. Pumchusak, The effect of surfactant concentration on the interlayer structure of organoclay, Chiang. Mai. J. Sci. 35 (2008) 199–204.

[43] J. Ma, B. Cui, J. Dai, D. Li, Mechanism of adsorption of anionic dye from aqueous solutions onto organobentonite, J. Hazard. Mater. 186 (2011) 1758–1765.

[44] D.M. Moore, C. Reynolds Jr, X-Ray Diffraction and the Identification and Analysis of Clay Minerals, 2nd ed. Oxford: Oxford University Press; 1997.

[45] A.S. Rajan, S. Sampath, A.K. Shukla, An in situ carbon-grafted alkaline iron electrode for iron-based accumulators, Energy Environ. Sci. 7 (2014) 1110–1116.

[46] T.J. Bandosz, K. Putyera, J. Jagieuo, J. A. Schwarz, Study of carbon-smectite composites and carbons obtained by in situ carbonization of polyfurfuryl alcohol, Carbon 32 (1994) 659-664.

[47] T. Kyotani, T. Mori, A. Tomita, Formation of a flexible graphite film from poly(acrylonitrile) using a layered clay film as template, Chem. Mater. 6 (1994) 2138-2142.

[48] C. Ruiz-García, J. Pérez-Carvajal, A. Berenguer-Murci, M. Darder, P. Aranda, D. Cazorla-Amorós, E. Ruiz-Hitzky, Clay-supported graphene materials: application to hydrogen storage, Phys. Chem. Chem. Phys. 15(2013) 18635-18641.

[49] P. Anadão, E. A. Hildebrando, I. L. R. Pajolli, K. R. de Oliveira Pereira, H. Wiebeck, F. R. V. Díaz, Montmorillonite/carbon nanocomposites prepared from sucrose for catalytic applications, Appl. Clay Sci. 53 (2011) 288-296.

[50] Q. Chen, R. Zhua, W. Deng, Y. Xub, J. Zhu, Q. Tao, H. He, From used montmorillonite to carbon monolayer–montmorillonite nanocomposites, Appl. Clay Sci. 100 (2014) 112-117.

[51] C. Xu, G. Ning, X. Zhu, G. Wang, X. Liu, J. Gao, Q. Zhang, W. Qian, F. Wei, Synthesis of graphene from asphaltene molecules adsorbed on vermiculite layers, Carbon 62 (2013) 213-221.

[52] N. Jović-Jovičić, A. Milutinović-Nikolić, M. Žunić, Z. Mojović, P. Banković, I. Gržetić, D. Jovanović, Synergic adsorption Pb2+ and reactive dye - RB5 on two series orgamonodified bentonites, J. Contam. Hydrol. 150 (2013) 1–11.

[53] N. Hamdi, E. Srasra, Acid-base properties of organosmectite in aqueous suspension, Appl. Clay Sci. 99 (2014) 1–6.

[54] E. Tombácz, M. Szekeres, Colloidal behavior of aqueous montmorillonite suspensions: the specific role of pH in the presence of indifferent electrolytes, Appl. Clay Sci. 27 (2004) 75–94.

[55] S. Lazarević, I. Janković-Častvan, D. Jovanović, S. Milonjić, Dj. Janaćković, R. Petrović, Adsorption of Pb^{2+}, Cd^{2+} and Sr^{2+} ions onto natural and acid-activated sepiolites, Appl. Clay Sci. 37 (2007) 47–57.

[56] A.C. Ferrari, Raman spectroscopy of graphene and graphite: Disorder, electron–phonon coupling, doping and nonadiabatic effects Solid State Communications 143 (2007) 47–57.

[57] P. K. Chu, L. Li, Characterization of amorphous and nanocrystalline carbon films, Materials Chemistry and Physics 96 (2006) 253–277.

[58] B.T. Mark, E. Orazem, Electrochemical Impedance Spectroscopy, New Jersey: John Wiley & Sons, Inc., 2008.

[59] E. Ngameni, I.K. Tonlé, J.T. Apohkeng, R.G.B. Bouwé, A.T. Jieumboué, A. Walcarius, Permselective and Preconcentration Properties of a Surfactant-Intercalated Clay Modified Electrode, Electroanalysis 18 (2006) 2243–2250.

[60] A. Fitch, Clay-modified electrodes: A Review, Clay Clay Miner. 38 (1990) 391–400.

[61] X. Li, J. Rong, B. Wei, Electrochemical behavior of single-walled carbon nanotube supercapacitors under compressive stress, ACS Nano 4 (2010) 6039–6049.

[62] D-J. Yun, H. Ra, S-W. Rhee, Concentration effect of multiwalled carbon nanotube and poly(3, 4-ethylenedioxythiophene) polymerized with poly(4-styrenesulfonate) conjugated film on the catalytic activity for counter electrode in dye sensitized solar cells, Renew. Energ. 50 (2013) 692–700.

[63] R.L. McCreery, Advanced Carbon Electrode Materials for Molecular Electrochemistry, Chem. Rev. 108 (2008) 2646–2687.

[64] A.J. Bard, Inner-Sphere Heterogeneous Electrode Reactions. Electrocatalysis and Photocatalysis: The Challenge, J. Am. Chem. Soc. 132 (2010) 7559–7567.

ACCEPTED MANUSCRIPT

Figure Captions

Figure 1. X-ray diffractograms of a) the Na-B and H series; b) C series (Sm – smectite, Q quartz, F – feldspar and C – calcite).

Figure 2: pH_f as a function of pH_i for selected samples. Equilibration time was 24 h. Background electrolyte 0.01 M KCl.

Figure 3: Raman spectra in the region of the typical D and G bands of C series samples

Figure 4: Electrochemical impedance spectra of electrodes with CB/clay ratio of 2:1 of: a) Na-B and samples of H series and b) CBP and samples of C series recorded at OCP in 1 mM $K_4[Fe(CN)_6]$ + 0.5 M KCl.

Figure 5: The equivalent electric circuit used to fit EIS data

Figure 6: Cyclic voltammograms of electrodes with CB/clay ratio of 2:1 of: a) Na-B and samples of H series and b) CBP and samples of C series recorded in 1 mM $K_4[Fe(CN)_6]$ +0.5 M KCl at scan rate of 50 mV s^{-1}.

Figure 7: SWV of 0.01 M Cu(II) using electrodes with CB/clay ratio of 2:1 of: a) Na-B and samples of H series and b) CBP and samples of C series.

Figure 8. Electrochemical impedance spectra of electrodes with CB/clay ratio of 1:9 of samples of C series recorded at OCP in 1 mM $K_4[Fe(CN)_6]$ + 0.5 M KCl.

Figure 9: SWV of 0.01 M Cu(II) using electrodes with CB/clay ratio of 1:9 of C series.

ACCEPTED MANUSCRIPT

Table 1: The selected textural properties of investigated samples

Na-B and H series						C series					
Sample	$S_{BET,}$ m^2/g	V_{tot}, cm^3/g	V_{mic}, cm^3/g	D_{med}, nm	D_{max}, nm	Sample	$S_{BET,}$ m^2/g	V_{tot}, cm^3/g	V_{mic}, cm^3/g	D_{med}, nm	D_{max}, nm
Na-B	118	0.121	0.048	3.9	4.0						
0.2H	20	0.050	0.016	4.0	4.6	0.2C	10	0.059	0.003	9.0	-
0.5H	19	0.045	0.009	4.1	4.6	0.5C	9	0.058	0.004	8.5	-
1.0H	3	0.021	-	4.7	7.1	1.0C	54	0.171	0.013	7.6	3.6
2.0H	-	-	-	-	-	2.0C	35	0.088	0.009	6.8	3.7
3.0H	-	-	-	-	-	3.0C	27	0.092	0.007	7.4	3.6

Where: S_{BET} – specific surface area, V_{tot} – total pore volume, V_{mic} –micropore volume, D_{med} – median pore diameter, D_{max} – the most abundant pore diameter

ACCEPTED MANUSCRIPT

Table 2: The electrochemical parameters obtained by fitting EIS data recorded using electrodes with CB/clay ratio of 2:1 in 1 mM $K_4[Fe(CN)_6]$+0.5 M KCl

Na-B and H series						CBP and C series					
Electrode	R_{ct} (kΩ)	Y_1 (μSs^{n1})	n1	Y_2 (nSs^{n2})	n2	Electrode	R_{ct} (MΩ)	Y_1 (μSs^{n1})	n1	Y_2 (nSs^{n2})	n2
Na-B	41.4	8.9	0.3	23	0.8	CBP	1.51	2.9	0.1	4.5	0.9
0.2H	92.2	6.4	0.3	13	0.8	0.2C	1.73	1.7	0.4	7.4	0.9
0.5H	7.9	13.8	0.4	25	0.8	0.5C	2.84	4.4	0.5	14.1	0.8
1.0H	3.2	15.7	0.4	115	0.7	1.0C	2.87	12.7	0.7	30.6	0.8
2.0H	3.0	37.5	0.4	895	0.6	2.0C	2.45	2.6	0.5	3.5	0.8
3.0H	2.2	33.4	0.3	1690	0.5	3.0C	2.70	2.9	0.4	2.6	0.9

ACCEPTED MANUSCRIPT

Table 3: The electrochemical parameters obtained by fitting EIS data recorded using electrodes with CB/clay ratio of 1:9 in 1 mM $K_4[Fe(CN)_6]$+0.5 M KCl

Electrode	R_{ct} (kΩ)	Y_1 (μSs^{n1})	n1	Y_2 (nSs^{n2})	n2
0.2C	415	1.72	0.3	51.3	0.7
0.5C	105	5.14	0.1	17.7	0.8
1.0C	100	1.19	0.1	10.6	0.8
2.0C	410	2.48	0.2	16.9	0.8
3.0C	370	2.79	0.2	16.4	0.8

ACCEPTED MANUSCRIPT

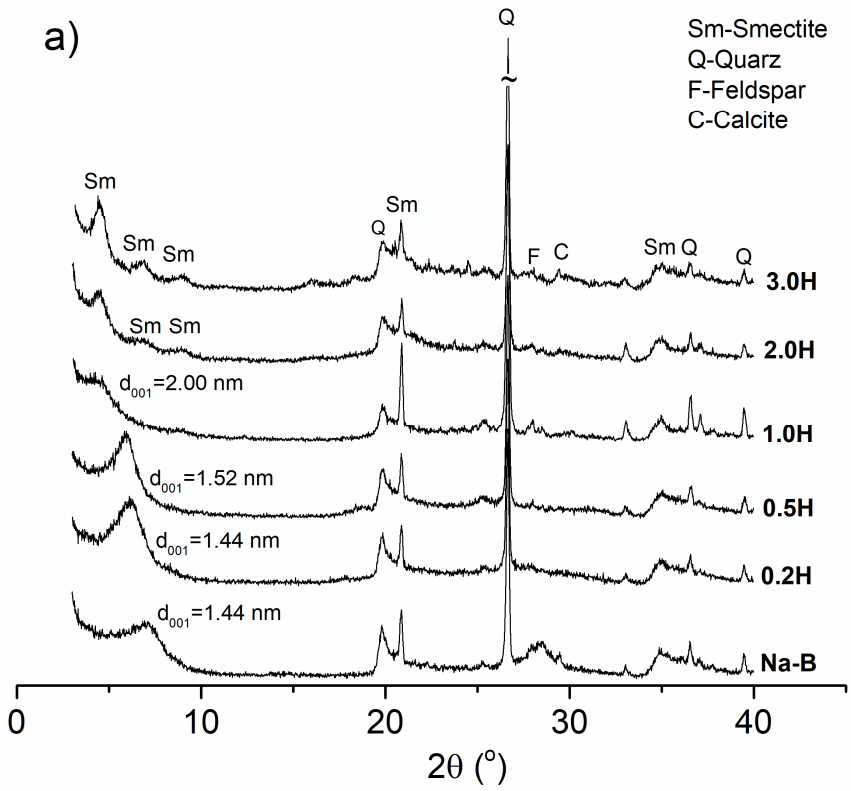

ACCEPTED MANUSCRIPT

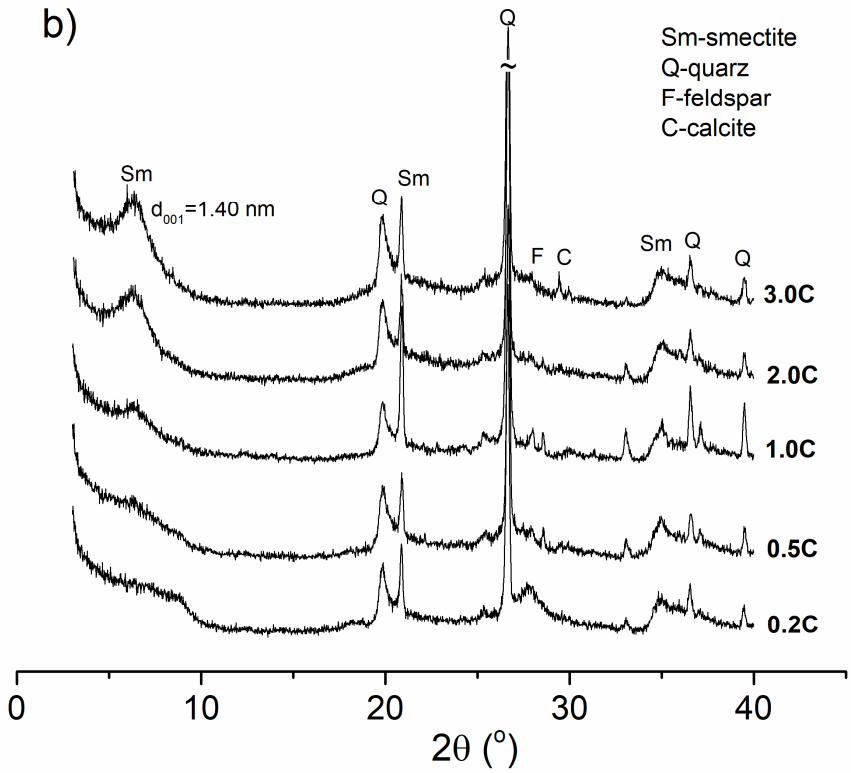

ACCEPTED MANUSCRIPT

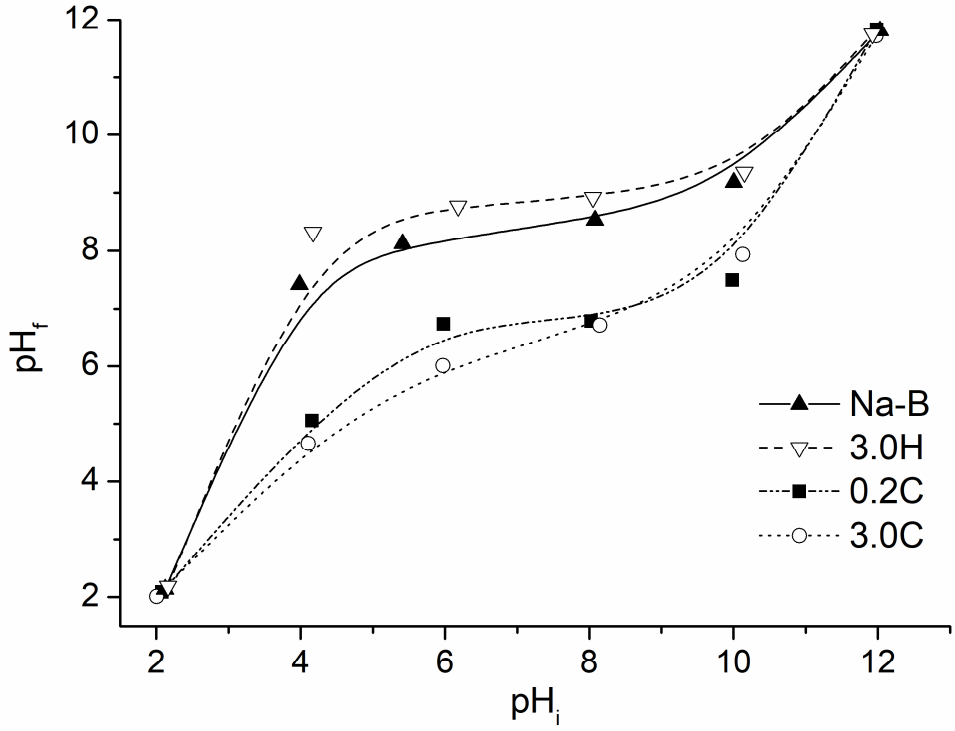

ACCEPTED MANUSCRIPT

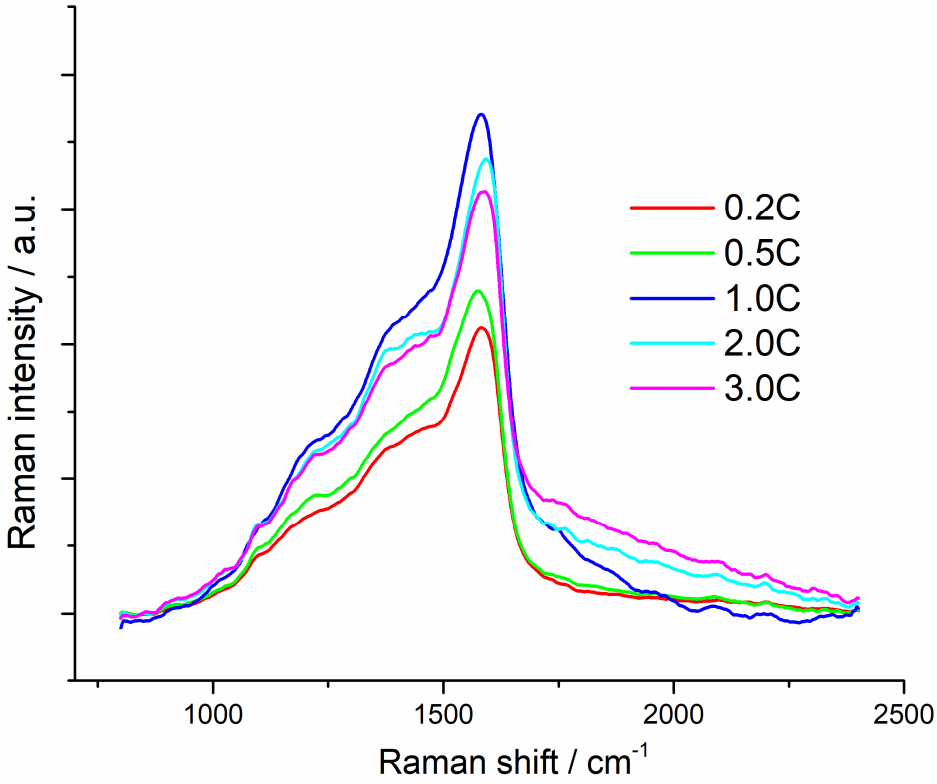

ACCEPTED MANUSCRIPT

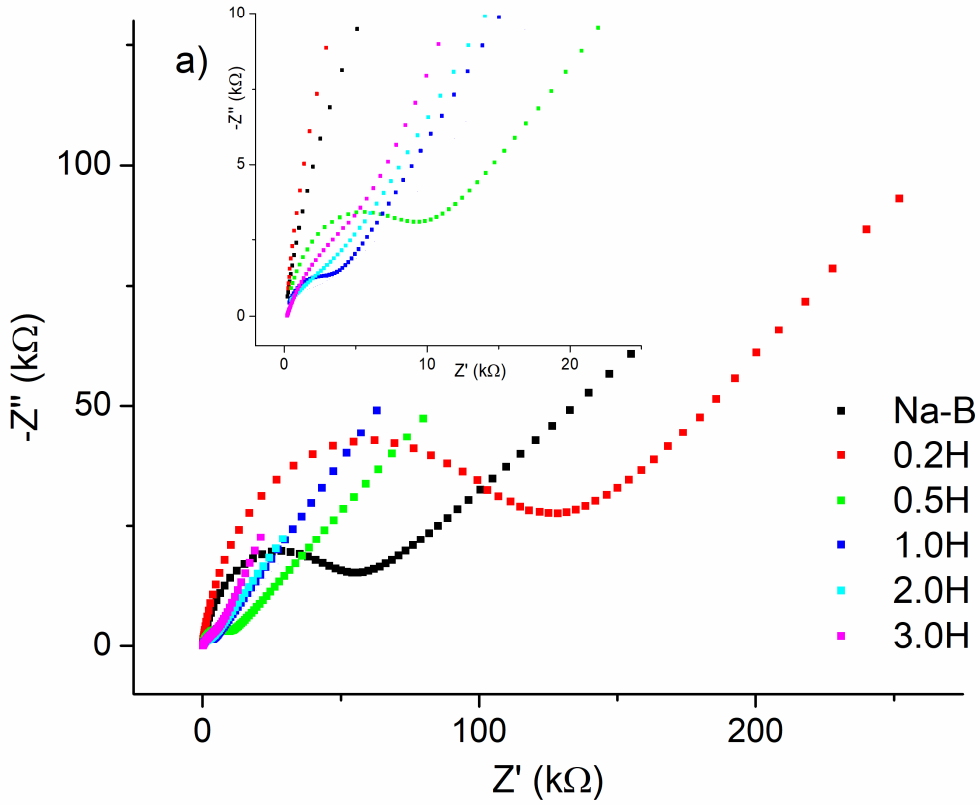

ACCEPTED MANUSCRIPT

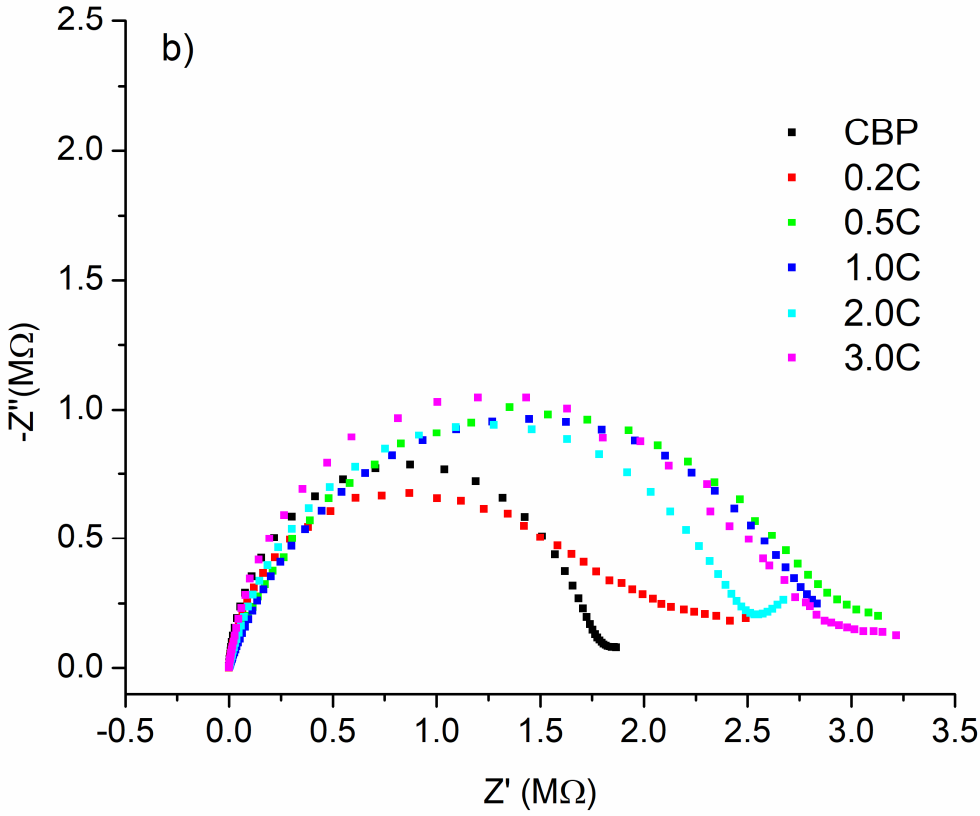

ACCEPTED MANUSCRIPT

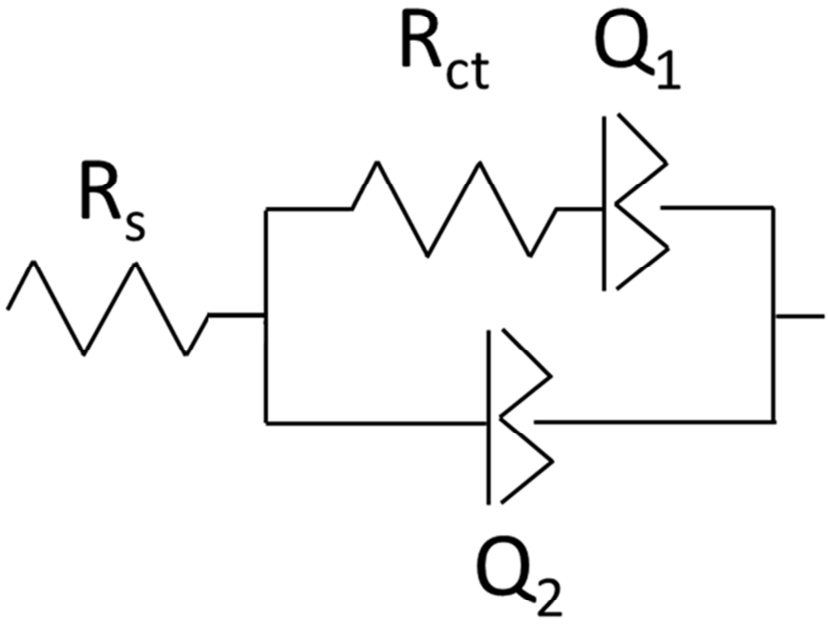

ACCEPTED

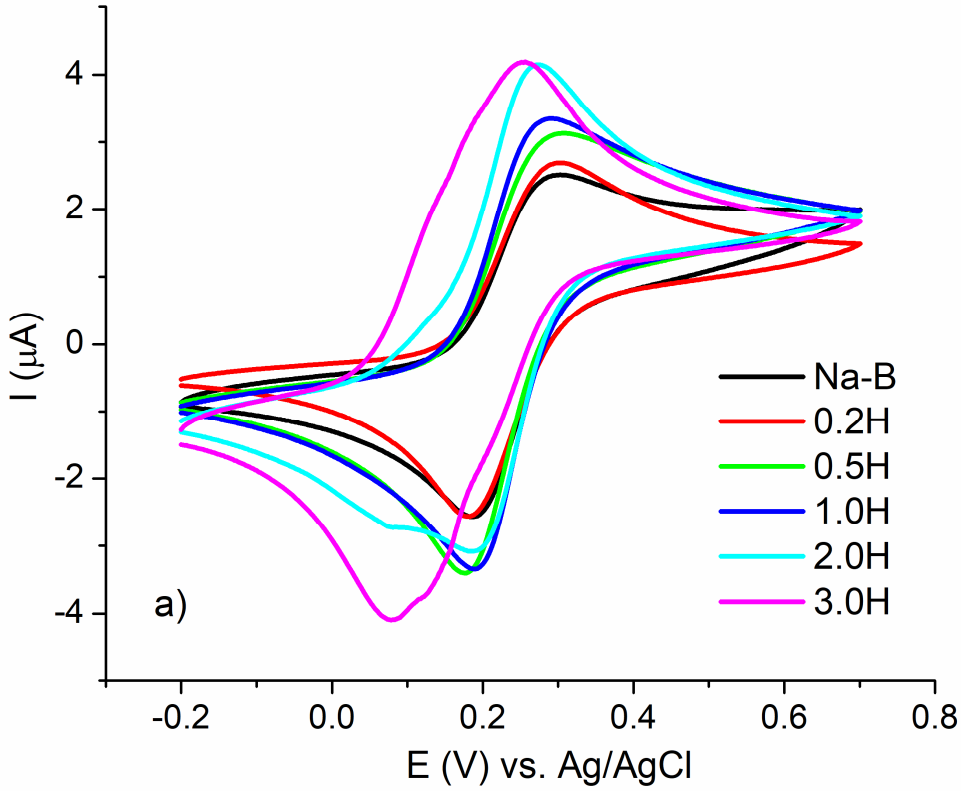

ACCEPTED MANUSCRIPT

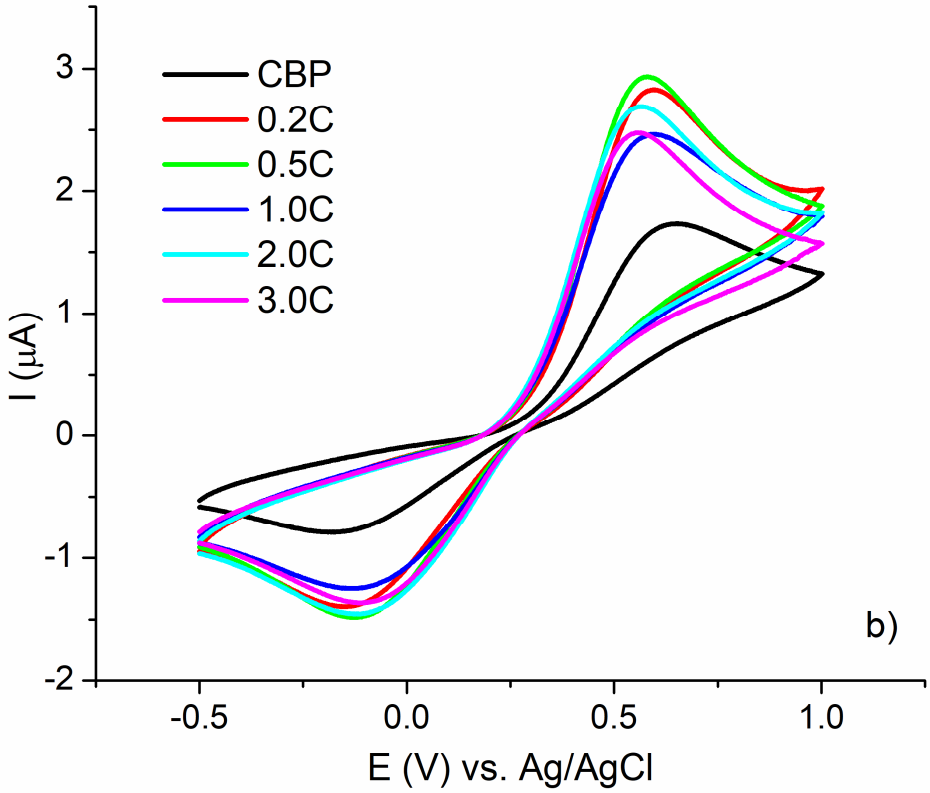

ACCEPTED MANUSCRIPT

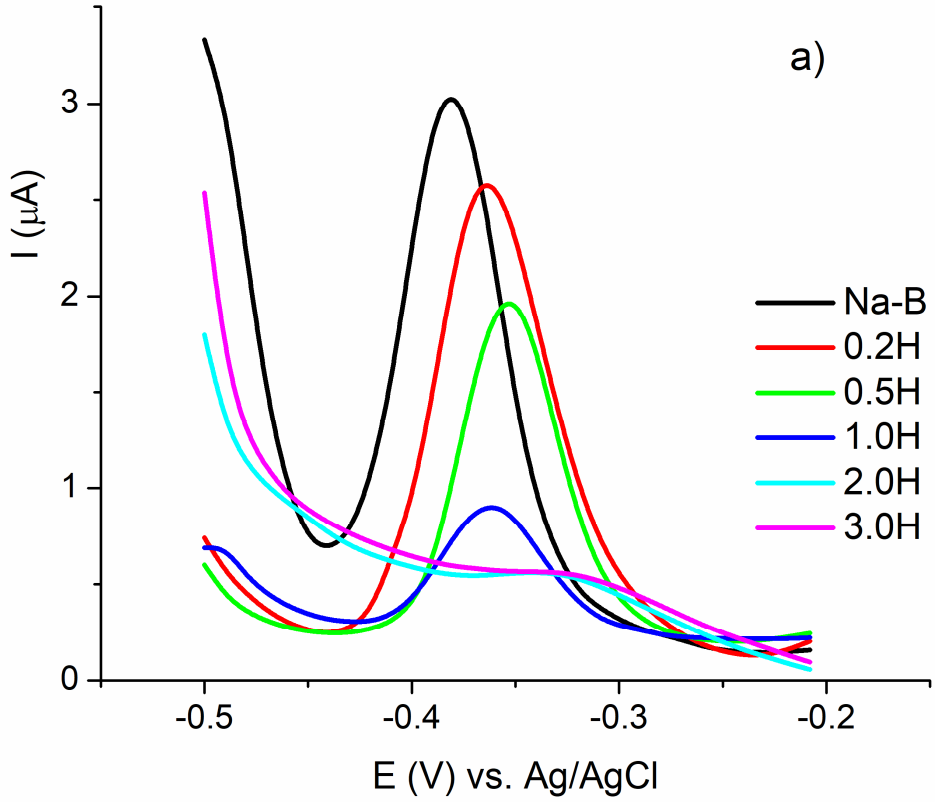

ACCEPTED MANUSCRIPT

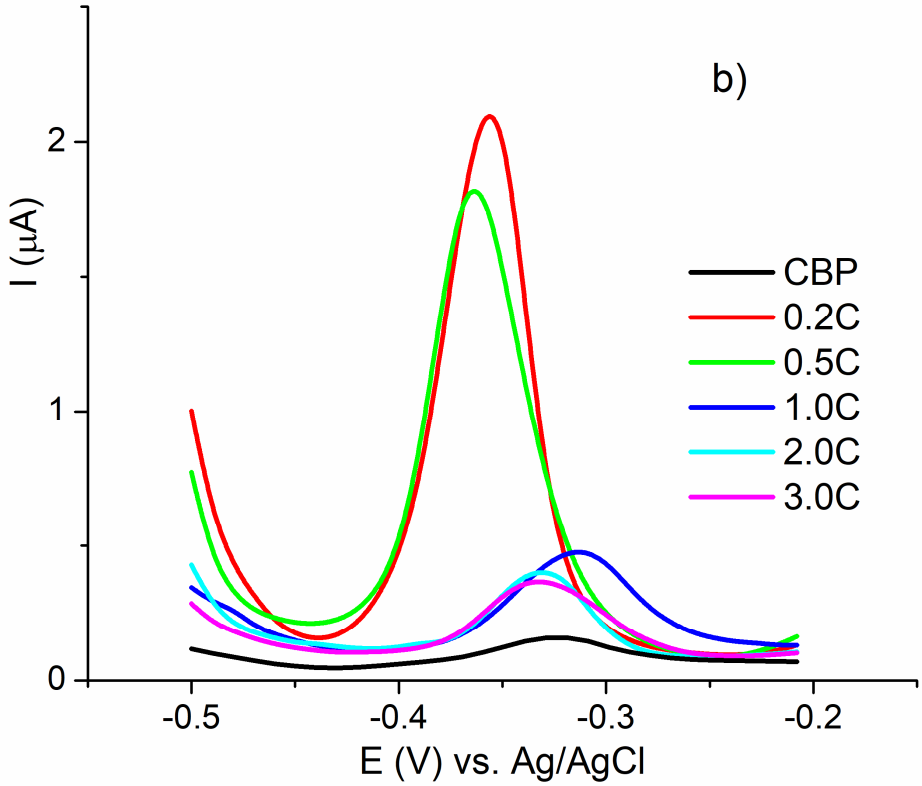

ACCEPTED MANUSCRIPT

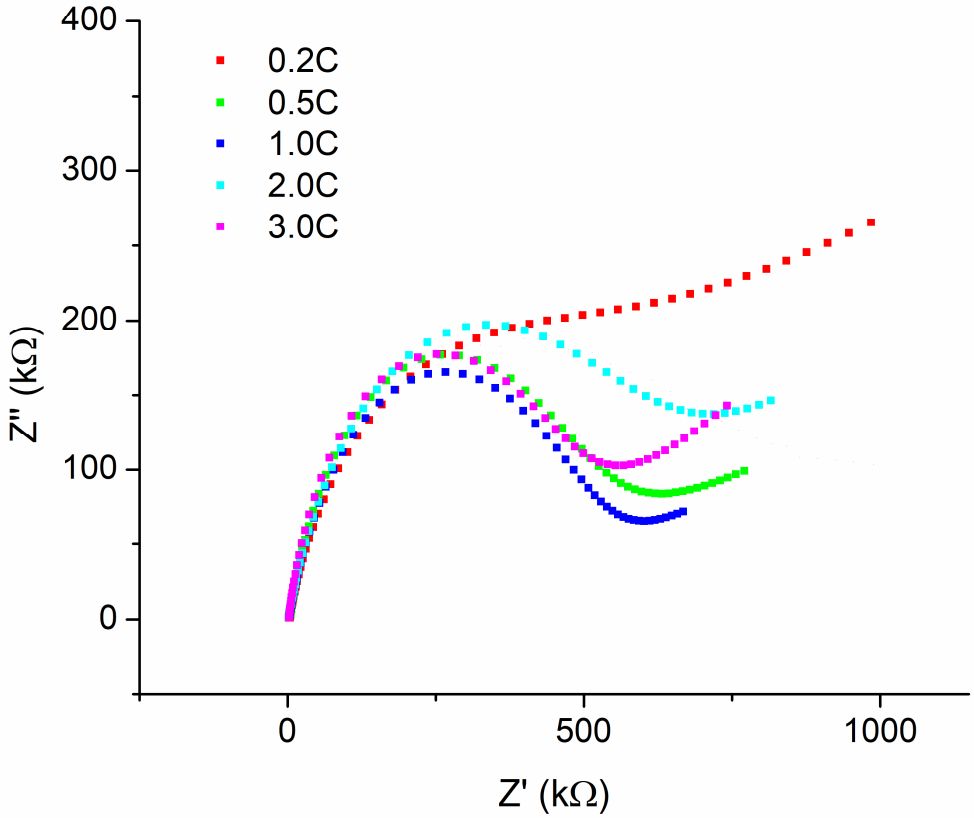

ACCEPTED MANUSCRIPT

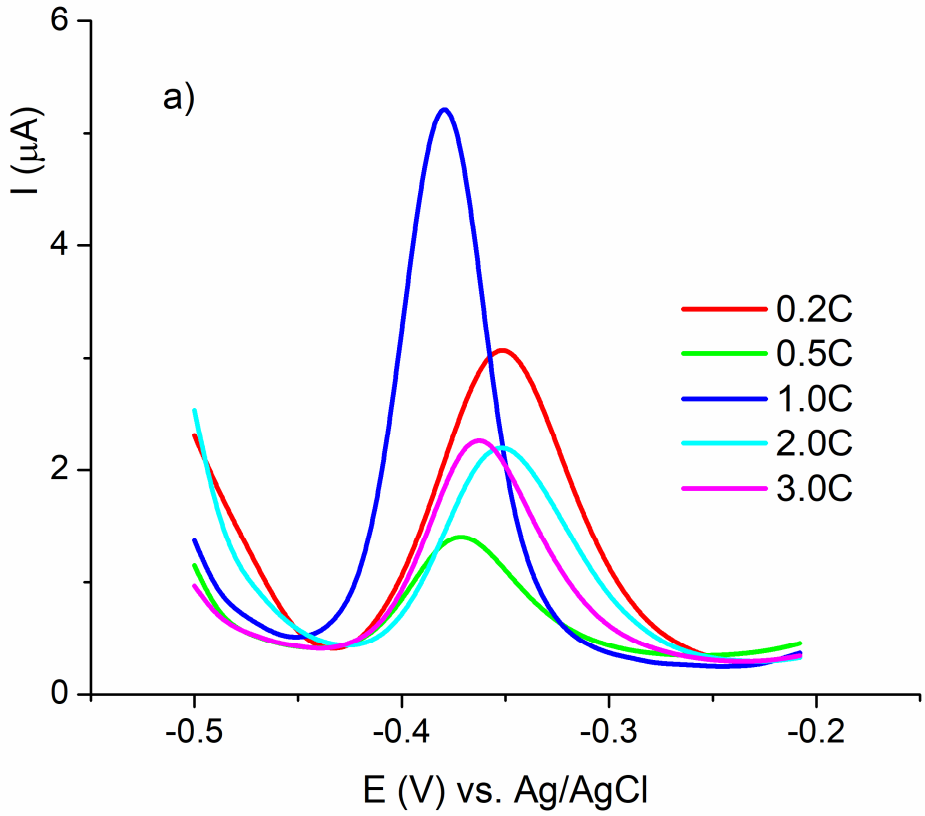

ACCEPTED MANUSCRIPT

ACCEPTED MANUSCRIPT

- Organoclays with different alkylammoinum/clay ratios were synthesized.
- Obtained organoclays were used as precursors for carbon-clay composite materials.
- Synthesized materials were used as modifiers of carbon paste electrode.
- The importance of interlamellar species for charge transfer process was evidenced.
- Carbon formed *in situ* influenced the performace of carbon-clay based electrodes.

ACCEPTED MANUSCRIPT